Journal of the American College of Cardiology Vol. 54, No. 12, 2009

Published by Elsevier Inc.

ISSN 0735-1097/09/$36.00
doi:10.1016/j.jacc.2009.06.014

Adenosine-Induced Stress Myocardial Perfusion Imaging Using Dual-Source Cardiac Computed Tomography

Ron Blankstein, MD,*† Leon D. Shturman, MD,* Ian S. Rogers, MD, MBA,* Jose A. Rocha-Filho, MD,* David R. Okada, MD,* Ammar Sarwar, MD,* Anand V. Soni, MD,* Hiram Bezerra, MD,*‡ Brian B. Ghoshhajra, MD, MBA,* Milena Petranovic, MD,* Ricardo Loureiro, MD,* Gudrun Feuchtner, MD,*§ Henry Gewirtz, MD,* Udo Hoffmann, MD, MPH,* Wilfred S. Mamuya, MD, PHD,*‖ Thomas J. Brady, MD,* Ricardo C. Cury, MD*¶

Boston and Brookline, Massachusetts; Cleveland, Ohio; Innsbruck, Austria; and Miami, Florida

Objectives This study sought to determine the feasibility of performing a comprehensive cardiac computed tomographic (CT) examination incorporating stress and rest myocardial perfusion imaging together with coronary computed tomography angiography (CTA).

Background Although cardiac CT can identify coronary stenosis, very little data exist on the ability to detect stress-induced myocardial perfusion defects in humans.

Methods Thirty-four patients who had a nuclear stress test and invasive angiography were included in the study. Dual-source computed tomography (DSCT) was performed as follows: 1) stress CT: contrast-enhanced scan during adenosine infusion; 2) rest CT: contrast-enhanced scan using prospective triggering; and 3) delayed scan: acquired 7 min after rest CT. Images for CTA, computed tomography perfusion (CTP), and single-photon emission computed tomography (SPECT) were each read by 2 independent blinded readers.

Results The DSCT protocol was successfully completed for 33 of 34 subjects (average age 61.4 ± 10.7 years; 82% male; body mass index 30.4 ± 5 kg/m^2) with an average radiation dose of 12.7 mSv. On a per-vessel basis, CTP alone had a sensitivity of 79% and a specificity of 80% for the detection of stenosis ≥50%, whereas SPECT myocardial perfusion imaging had a sensitivity of 67% and a specificity of 83%. For the detection of vessels with ≥50% stenosis with a corresponding SPECT perfusion abnormality, CTP had a sensitivity of 93% and a specificity of 74%. The CTA during adenosine infusion had a per-vessel sensitivity of 96%, specificity of 73%, and negative predictive value of 98% for the detection of stenosis ≥70%.

Conclusions Adenosine stress CT can identify stress-induced myocardial perfusion defects with diagnostic accuracy comparable to SPECT, with similar radiation dose and with the advantage of providing information on coronary stenosis. (J Am Coll Cardiol 2009;54:1072–84) © 2009 by the American College of Cardiology Foundation

Although cardiac computed tomography (CT) has shown very good diagnostic accuracy for the detection of coronary artery disease (CAD), the physiologic significance of many lesions can be uncertain (1). Furthermore, the presence of calcified atherosclerotic plaque reduces the ability to differentiate significant stenosis from nonobstructive plaque.

See page 1085

Thus, invasive angiography or perfusion imaging by single-photon emission computed tomography (SPECT), positron emission tomography, or magnetic resonance imaging (MRI) are often better suited for accurately identifying obstructive or physiologically significant disease in these patients.

From the *Cardiac MR PET CT Program, Department of Radiology and Division of Cardiology, Massachusetts General Hospital and Harvard Medical School, Boston, Massachusetts; †Noninvasive Cardiovascular Imaging Program, Department of Medicine and Radiology, Brigham and Women's Hospital, Boston, Massachusetts; ‡Harrington McLaughlin Heart and Vascular Institute, Case Western Reserve University, Cleveland, Ohio; §Department of Radiology, Innsbruck Medical University, Innsbruck, Austria; ‖Lown Cardiovascular Group, Brookline, Massachusetts; and the ¶Cardiovascular MR and CT Program, Baptist Cardiac and Vascular Institute, Miami, Florida. This study was supported in part by a grant from Astellas, Inc. Drs. Blankstein, Shturman, Rogers, and Soni have received support from National Institutes of Health grant 1T32 HL076136. Dr. Hoffmann has received research grants from GE Healthcare, Bracco Diagnostics, and Bayer Healthcare. Dr. Cury has received research grant support from Astellas Pharma, Inc.

Manuscript received February 2, 2009; revised manuscript received May 18, 2009, accepted June 2, 2009.

Extensive data regarding the prognostic value of myocardial perfusion imaging (MPI) have shown that the amount of infarcted and ischemic burden correlates with long-term outcomes and can help decide which patients are best suited for revascularization versus medical therapy (2,3). It follows that the ability to combine anatomical data from computed tomography angiography (CTA) together with the physiological significance provided by perfusion may be beneficial (4,5).

The ability of CT to identify rest myocardial perfusion defects (i.e., areas of myocardial infarction) has been shown in both animal and human studies (6–10). Such studies have shown that areas of hypoenhanced regions on multidetector CT correspond directly to perfusion defects visualized on MRI and areas of myocardial infarction seen on triphenyl tetrazolium chloride staining. These and other studies showed that iodinated contrast agents used in CT have similar kinetics to gadolinium used in MRI (11). Thus, imaging performed immediately after contrast administration shows areas of hypoenhancement corresponding to a perfusion defect (i.e., delayed wash-in of contrast) and delayed imaging acquired 5 to 10 min after contrast administration may show regional delayed hyperenhancement corresponding to areas of myocardial necrosis or scar (i.e., delayed wash-out of contrast) (11). More recently, animal models of stenosis and preliminary human studies have shown that CT can also diagnose areas of ischemic myocardium under adenosine-induced stress (12–14).

The feasibility and accuracy of performing a comprehensive CT examination incorporating coronary imaging, stress and rest myocardial perfusion, and delayed enhancement (DE) imaging in humans is unknown. Therefore, we sought to determine the feasibility and diagnostic accuracy of adenosine mediated stress dual-source computed tomography (DSCT) in identifying hemodynamically significant stenosis as compared with nuclear MPI using invasive angiography as the reference standard.

Methods

Patient population. Eligible participants for the study included 767 consecutive patients in our institution who were ≥40 years of age, underwent a nuclear stress test, and were referred for or had a high likelihood to undergo invasive angiography. Assessment for eligibility was based on screening the following 2 populations: 1) all patients scheduled to undergo clinically indicated invasive angiography who have had a prior nuclear MPI within the previous 3 months; and 2) all patients who underwent nuclear MPI and were found to have high-risk features (i.e., high likelihood to be referred for invasive angiography). Reasons for exclusion included unstable clinical status, acute coronary syndrome, asthma, critical aortic stenosis, and known allergy to iodinated contrast. Figure 1 summarizes the patient flow and specific reasons for exclusions. The CT results were blinded and were not provided to the referring physician, and thus did not influence the decision to undergo cardiac catheterization. The study was approved by an institutional review board (Partners Health Care System), and all subjects gave informed consent.

Abbreviations and Acronyms

CAD = coronary artery disease
CT = computed tomography
CTA = computed tomography angiography
CTP = computed tomography perfusion
DE = delayed enhancement
DSCT = dual-source computed tomography
MPHR = maximal predicted heart rate
MPI = myocardial perfusion imaging
MRI = magnetic resonance imaging
SPECT = single-photon emission computed tomography

Image acquisition: comprehensive CT protocol. Patients were instructed not to consume any caffeine for at least 24 h before the scan. On arrival, 2 intravenous lines were inserted (18 gauge for contrast delivery; 20 gauge for adenosine infusion). Given that commonly used medications in cardiac CT (i.e., nitroglycerin, beta-blockers) may have an impact on myocardial perfusion (15), no medication other than adenosine was administered.

The CT was performed on the 64-slice DSCT scanner (Definition, Siemens Medical Systems, Forchheim, Germany) with a gantry rotation time of 330 ms. A flying focus along the z-axis (z-sharp technology) was used to acquire 64 overlapping 0.6-mm slices using two 32-detector rows. The resulting temporal resolution was 83 ms.

Figure 2 shows the CT protocol involving the stress, rest, and DE acquisitions. After scout images were obtained, contrast timing was determined with the use of a test bolus of 10 to 15 ml of contrast. Flow rate for the test bolus and for image acquisition was typically 4 to 5 ml/s and was followed by a 20-ml flush of saline. Subsequently, for both the stress and rest scans, image acquisition timing was determined by adding 2 to 4 s to the time of peak contrast enhancement in the ascending aorta to allow perfusion of the myocardium.

After the test bolus, adenosine infusion was started at 140 μg/kg/min. A retrospectively gated scan with tube current modulation and pitch adaptation was obtained 3 min after the initiation of the infusion. Tube voltage (kV) and current (mAs) were chosen based on the patient's body habitus. Although 120 kV was used for the majority of patients, 100 kV was used for those with a body mass index <30 kg/m^2 who were nonobese (i.e., weight <220 lbs).

Typical contrast dose for this portion of the examination was 65 ml of iopamidol delivered at a rate of 4 to 5 ml/s. Throughout the infusion, patient symptoms, heart rate, blood pressure, and electrocardiogram were monitored by a cardiologist. Table 1 summarizes the CT scan parameters.

Immediately after the stress CT, the adenosine infusion was discontinued. On symptom resolution and return of heart rate to baseline (typically 5 min), the rest CT scan was obtained. To reduce radiation exposure, rest CT used

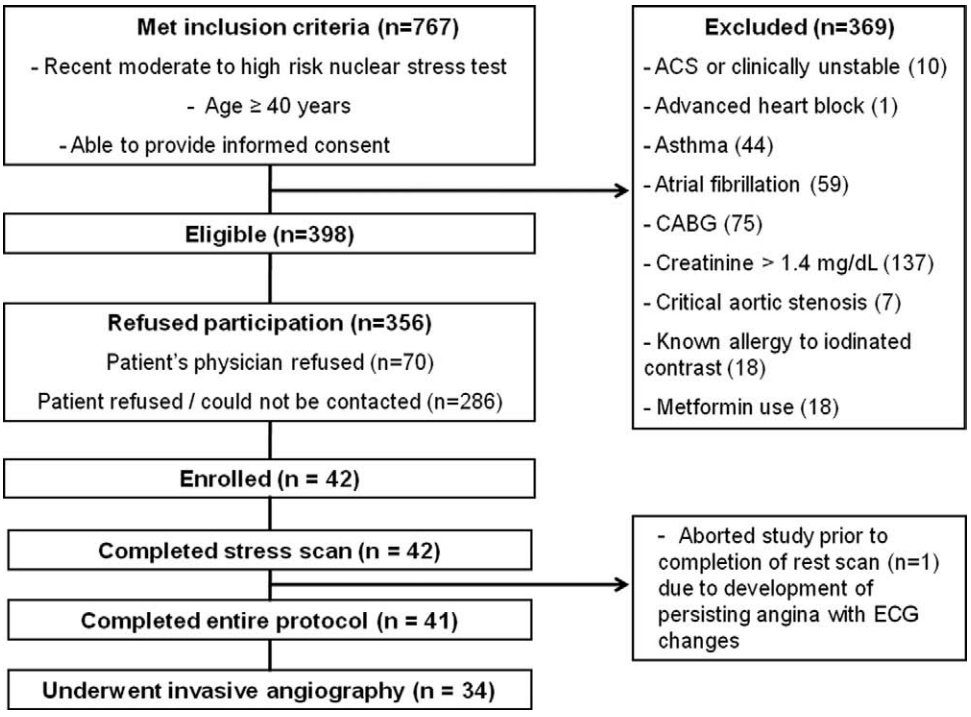

Figure 1 **Flow Diagram of Patients Eligible for Recruitment and Reasons for Exclusion**

Of 767 patients meeting inclusion criteria, 369 were excluded; 42 patients completed the computed tomography (CT) stress perfusion scan, out of which 34 also underwent invasive angiography. ACS = acute coronary syndrome; CABG = coronary artery bypass grafting surgery; ECG = electrocardiogram.

prospective triggering (Sequential Scanning, Siemens Medical Systems) at 65% of the RR interval (16). The rest CT used the same tube voltage and a similar tube current as the stress scan. As was also the case for the stress CT scan, tube current was chosen individually for each patient based on body habitus. The typical contrast dose for this portion of the examination was 65 to 75 ml of iopamidol delivered at a rate of 4 to 5 ml/s.

To detect areas of DE, a third scan was then performed 7 min after the rest scan. The following actions were used to reduce radiation dose: 1) 100 kV for all but 1 patient, who received 80 kV; 2) collimation was increased from 0.6 to 1.2 mm; and 3) prospective triggering at 65% of the RR interval. The tube current (mA) used for the DE scan was similar to the value chosen for the rest scan.

Nuclear stress testing. All nuclear SPECT examinations were performed according to standard institutional clinical protocols. Among the 34 study participants, 12 underwent adenosine SPECT MPI, whereas the remaining 22 had exercise SPECT MPI. Among the 22 exercise stress tests, the average exercise time was 7 min and 10 s and the average workload achieved was 7.8 METs. The average percent of maximal predicted heart rate (MPHR) was 85.2%. Thirteen patients (3 of whom had ≤85% MPHR) developed chest pain during the examination.

An adequate stress test was defined as: 1) achieving ≥85% of MPHR; 2) any test using adenosine; or 3) patient developing chest pain during exercise testing. Although only 54% of exercise tests achieved MPHR ≥85%, 79% of stress tests were considered adequate. None of the patients who failed to achieve an adequate test had significant electrocardiogram changes during exercise.

Patients were injected with 10 mCi of ^{99m}Tc sestamibi at rest, and SPECT images were acquired with a dual-detector gamma camera, with 64 projections, each for 20 s, in a noncircular 180° orbit. In addition, an exercise or pharmacological stress test (intravenous adenosine infusion at 140 μg/kg/min for 5 min) was performed with 30 mCi of ^{99m}Tc sestamibi. After 30 to 60 min, gated SPECT images were obtained and assessed for myocardial perfusion.

Image processing and interpretation. SPECT MPI. All SPECT MPI images were analyzed by 2 experienced Certification Board of Nuclear Cardiology-certified independent readers (L.S. and W.M.), and any areas of discrepancy were then resolved by a third experienced senior reader (H.G.). Using the 17-segment model recommended by the American College of Cardiology/American Heart Association/American Society of Nuclear Cardiology (17), semiquantitative visual assessment of myocardial perfusion was performed using a 4-point scoring system (0 = normal, 1 = mild reduction of radioisotope uptake, 2 = moderate reduction of radioisotope uptake, 3 = severe reduction of radioisotope uptake). For each patient, summed rest score and

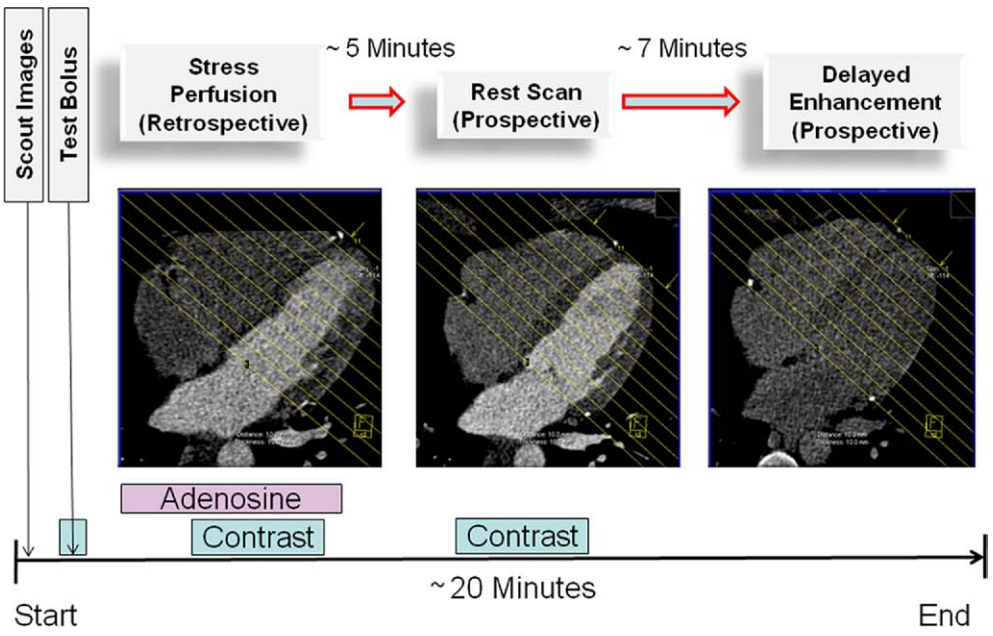

Figure 2 Comprehensive Computed Tomography Protocol

See the Methods section for detailed explanation. After scout images and test bolus were performed, adenosine infusion was started at 140 μg/kg/min. Three minutes later, a contrast-enhanced stress perfusion scan was acquired using retrospective gating and tube current modulation. Once the heart rate returned to baseline, the rest perfusion scan was acquired. This was a contrast-enhanced scan using prospective triggering. Approximately 7 min later, a low tube voltage, prospectively triggered delayed enhancement scan was acquired.

summed stress score were calculated by adding the corresponding scores of the 17 segments for the rest and stress images.

Table 1 CT Perfusion Scan Parameters

Parameter	Stress/ CT Angiography	Rest	DE
Image quality (using subjective 1–4 scale)	3.1 ± 0.7	3.4 ± 0.7	2.8 ± 0.8
Heart rate (beats/min)			
Minimum	73 ± 15	59 ± 11	61 ± 12
Maximum	87 ± 17	78 ± 16	80 ± 17
Mean	79 ± 13	68 ± 11	68 ± 12
Mean variability (maximum − minimum)	14 ± 19	19 ± 16	20 ± 18
Scan acquisition time (s)	7 ± 3	11 ± 3	7 ± 2
Pitch	0.36 ± 0.08	—	—
kV	116 ± 8	116 ± 8	100 ± 5
mAs (stress)/mA* (rest and DE)	339 ± 7	181 ± 34	183 ± 20
CT dose index volume	34.8 ± 13.8	9.5 ± 2.7	5.8 ± 1.6
Scan length (cm)	15.6 ± 2.7	12.6 ± 1.8	12.7 ± 1.7
Dose length product	537 ± 228	119 ± 35	73 ± 19
Effective radiation exposure (mSv)	9.1 ± 3.9	2.0 ± 0.6	1.2 ± 0.3
Contrast dose (ml)	65 ± 3	67 ± 3	0.0 ± 0.0

*For retrospective triggering (helical scanning), mAs = total tube current X gantry rotation time [~0.33s]; for prospective triggering (sequential scanning), mA = total tube current X exposure time [~0.2s].
CT = computed tomography; DE = delayed enhancement.

INVASIVE ANGIOGRAPHY. All invasive coronary angiography images were sent to an offsite core laboratory (Harrington McLaughlin Heart and Vascular Institute, Case Western Reserve University, Cleveland, Ohio), where blinded quantitative coronary assessment was performed for the entire coronary system (CAAS II system, Pie Medical, Maastricht, the Netherlands) to determine the percent stenosis of each coronary segment.

COMPUTED TOMOGRAPHY PERFUSION (CTP). Before evaluation of perfusion, raw data were used to reconstruct stress, rest, and DE datasets at 65% of the RR interval using an extra smooth filter (Siemens B10) with slice thickness of 0.7 mm and overlap of 0.4 mm.

To ensure appropriate and consistent coregistration of all images, internal fiducial markers (e.g., mitral annular ring, left ventricular apex, pulmonary vasculature) and spatial localization coordinates available in the software (Circulation, Siemens) were used to coregister the stress, rest, and DE images.

For each dataset, a double oblique technique was used to create true short-axis, 10-mm-thick multiplanar reformats images. Thicker slices were chosen because the increased voxel size results in decreased image noise and improves contrast resolution for visualization of normal and ischemic/infarcted myocardium.

For assessment of CTP analysis, the standard American College of Cardiology/American Heart Association

17-segment model was used. Semiquantitative per-segment analysis was performed by simultaneous visualization of short-axis images obtained from stress, rest, and delayed acquisitions. Narrow window and level settings were used (typically W200, L100), although the reading physician was allowed to adjust these display settings as needed.

After initial evaluation of thick multiplanar reformat short-axis images, readers were allowed to examine multiphase cine data from the stress CT scan (available in 2-chamber, 4-chamber, and short-axis views). Subsequently, global and regional wall motion abnormalities were noted. In addition, any areas of questionable perfusion defects were examined in both systolic and diastolic phases to differentiate potential artifacts (e.g., defect only present on 1 phase) from true perfusion defects (e.g., defect present on multiple phases and can be seen during both systole and diastole) and potentially associated to an area of regional wall motion abnormality (6,18). By using this methodology, approximately 20% of potential defects were ultimately classified as artifacts.

All CT stress, rest, and DE images were independently analyzed by 2 experienced readers (R.B. and R.C.C.) who were blinded to all patient and clinical data, including CT coronary angiographic findings. A joint consensus reading session was then performed to resolve any discrepancies, and consensus was achieved in all cases.

Each of the 17 segments was scored based on the absence or presence of a perfusion defect. Perfusion defect severity was graded as transmural (>50%) versus nontransmural (<50%). Reversibility was defined as follows: 0 = none, 1 = minimal, 2 = partial, 3 = complete.

For each dataset (i.e., stress, rest, DE), image quality was determined by use of a subjective scale: 1 = poor, 2 = moderate, 3 = good, 4 = excellent.

CTA. Raw data obtained during the stress CT was used to reconstruct images at every 10% of the cardiac cycle length using a standard cardiac filter (Siemens B26f) with slice thickness of 0.7 mm and overlap of 0.4 mm. The resulting multiphase dataset was used for CTA analysis. Of note, by design, our rest acquisition was optimized solely for the evaluation of myocardial perfusion (i.e., no nitroglycerin was administered because it has the potential to alter perfusion hemodynamics [15] and data were acquired during a single narrow phase of 65%).

The CTA analysis was performed by 2 experienced readers (L.S. and I.R.) who were blinded to all patient and clinical data, including CT and SPECT perfusion data. Whenever joint agreement could not be achieved, consensus was established by use of a third senior reader (R.C.C.). Each segment was graded as follows: 0 = normal, 1 = mild disease (1% to 40%), 2 = moderate disease (41% to 70%), 3 = significant stenosis or occluded (71% to 100%), or 4 = uninterpretable. Subjective image quality (1 = poor, 2 = moderate, 3 = good, 4 = excellent) was noted for each segment.

Matching of perfusion-based segments to corresponding vascular territory. To ensure correct association of the 17 myocardial segments with the correct vascular territory, angiographic visualization of vessel dominance was used to decide which vessel supplies the inferior and inferoseptal territories. In addition, depending on whether obtuse marginal or diagonal branches supplied the anterolateral wall, either the left circumflex or left anterior descending vessel was designated as supplying the basal and mid anterolateral wall.

Determination of reference standard. For all patients, obstructive CAD on invasive angiography (stenosis

Table 2 Baseline Characteristics of Patients

Characteristics	Total (n = 34)
Risk factor/demographics	
Age (yrs)	61.4 ± 10.7
Male sex (%)	82.4
Diabetes mellitus (%)*	32.4
Hypertension (%)	88.2
Dyslipidemia (%)*	85.3
Obesity (BMI ≥30 kg/m^2) (%)	41.2
Family history of CAD (%)*	50.0
Weight (lbs)	201.3 ± 35.5
BMI (kg/m^2)	30.4 ± 5.4
Smoking status (%)	
Current	17.7
Never	29.4
Former	52.9
Ethnicity (%)	
Caucasian	79.4
Black	14.7
Hispanic	5.9
Prior medical history (%)	
Previous angina	64.7
Prior myocardial infarction	35.3
Peripheral vascular disease	5.9
Prior CVA	0.0
Prior coronary revascularization	38.2
Biomarkers/lipids (mg/dl)	
Total cholesterol	164.1 ± 62.1
HDL cholesterol	46.0 ± 18.7
LDL cholesterol	104.4 ± 42.9
Serum triglycerides	149.4 ± 76.0
Serum creatinine	1.1 ± 0.2
Baseline medications (%)	
Aspirin	64.7
Beta-blocker	70.6
Statin	79.4
Vital signs	
Systolic blood pressure (mm Hg)	137.4 ± 19.5
Diastolic blood pressure (mm Hg)	76.9 ± 9.6
Heart rate (beats/min)	68.4 ± 12.3

*Family history, diabetes, and dyslipidemia classified per documentation in cardiologist note.
BMI = body mass index; CAD = coronary artery disease; CVA = cerebrovascular accident; HDL = high-density lipoprotein; LDL = low-density lipoprotein.

≥50% or 70%) was defined as the primary reference standard against which CTP and SPECT-MPI were compared.

Recognizing the limitations of comparing perfusion defects with anatomical stenosis, CTP was compared with SPECT MPI. Moreover, the following additional reference standards were tested: 1) any vessel that had ≥50% stenosis and a corresponding perfusion defect; and 2) any vessel that had ≥50% stenosis or a corresponding perfusion defect.

Radiation dose. Effective radiation dose for each component of the DSCT examination (stress, rest, and DE) was calculated by multiplying the dose-length product provided by scan console by a constant (k = 0.017 mSv/mGy/cm). To estimate radiation dose for SPECT MPI, total megabecquerel was converted to millisievert.

Statistical analysis. Data analysis was performed using Stata IC version 10.0 (StataCorp LP, College Station, Texas). All continuous variables were expressed as mean ± SD, whereas categorical variables were expressed as percentage. Differences in continuous variables were assessed using Student paired *t* tests. The McNemar test was used to calculate differences between proportions (i.e., sensitivity and specificity) obtained from paired observations. The area under the receiver-operator characteristic curve (C-statistic) was calculated for all diagnostic testing strategies for which a gold standard was available. The C-statistics were compared using the ROCCOMP statistic (StataCorp LP). A p value <0.05 was considered statistically significant.

Results

Patient population. Among the 34 study participants, the average age was 61.4 ± 10.7 years, 82% were male, 32% had diabetes, 88% had hypertension, and 85% had dyslipidemia. The prevalence of obesity was 41%, and the average body mass index was 30.4 ± 5.4 kg/m^2. There was a high prevalence of CAD: 64% had documented history of angina, 35% had a prior myocardial infarction, and 38% had a prior revascularization procedure (Table 2).

Invasive angiography. On invasive angiography, 25 (74%) patients had ≥50% stenosis and 17 (50%) patients had ≥70% stenosis in at least 1 coronary vessel. When considering the extent of disease, 13 (38%) patients had single-vessel disease, 7 (21%) had double-vessel disease, and 5 (15%) had triple-vessel disease. On a per vessel basis, 41% of the 102 vessels studies had ≥50% stenosis, whereas 22% had ≥70% stenosis.

SPECT MPI findings. On SPECT MPI, 26 (76%) of the 34 patients and 38 (37%) of the 102 vascular territories had perfusion abnormalities during stress. Of 38 vascular territories with abnormal SPECT MPI, 9 (24%) were fixed, 15 (39%) were fully reversible, and 14 (37%) were partially reversible. The average summed stress score was 5.5, and the average summed rest score was 2.9.

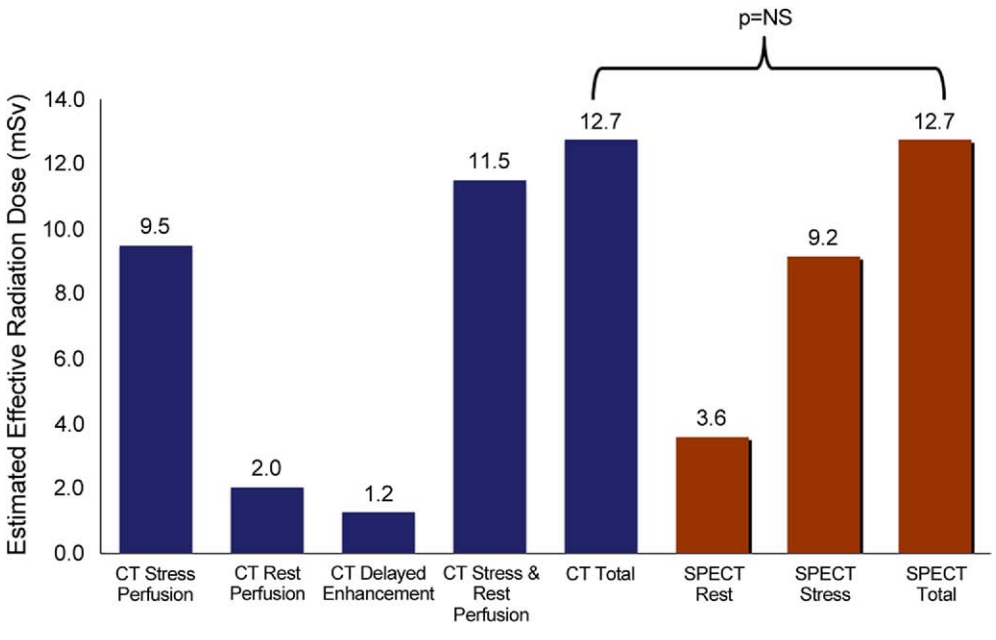

Figure 3 Radiation Exposure of Stress Cardiac CT Versus SPECT MPI

Estimated effective radiation dose in milisiverts (mSv) is shown for cardiac computed tomography (CT) **(blue bars)** and single-photon emission computed tomography (SPECT) myocardial perfusion imaging (MPI) **(red bars)**. The total effective radiation dose was equivalent for the 2 modalities.

JACC Vol. 54, No. 12, 2009
September 15, 2009:1072–84

Table 3 Per Vessel and Per Patient Diagnostic Accuracy of CT Perfusion and SPECT MPI

	Per Patient	Per Vessel
CT perfusion versus invasive angiography stenosis ≥50%		
Invasive angiography		
≥50% (+)	23	33
≥50% (−)	2	9
<50% (+)	3	12
<50% (−)	6	48
Sensitivity	0.92 (0.74–0.99)	0.79 (0.63–0.90)
Specificity	0.67 (0.30–0.93)	0.80 (0.68–0.89)
PPV	0.89 (0.70–0.98)	0.73 (0.58–0.85)
NPV	0.75 (0.35–0.97)	0.84 (0.72–0.93)
C-statistic	0.793	0.793
SPECT versus invasive angiography stenosis ≥50%		
Invasive angiography		
≥50% (+)	23	28
≥50% (−)	2	14
<50% (+)	3	10
<50% (−)	6	50
Sensitivity	0.92 (0.74–0.99)	0.67 (0.51–0.80)
Specificity	0.67 (0.30–0.93)	0.83 (0.72–0.92)
PPV	0.89 (0.70–0.98)	0.74 (0.57–0.87)
NPV	0.75 (0.35–0.97)	0.78 (0.66–0.88)
C-statistic	0.793	0.750
CT perfusion versus invasive angiography stenosis ≥70%		
Invasive angiography		
≥50% (+)	16	19
≥50% (−)	1	3
<50% (+)	10	26
<50% (−)	7	54
Sensitivity	0.94 (0.71–1.00)	0.86 (0.65–0.97)
Specificity	0.41 (0.18–0.67)	0.68 (0.56–0.78)
PPV	0.62 (0.41–0.80)	0.42 (0.28–0.58)
NPV	0.88 (0.47–1.00)	0.95 (0.85–0.99)
C-statistic	0.676	0.769
SPECT versus invasive angiography stenosis ≥70%		
Invasive angiography		
≥50% (+)	16	16
≥50% (−)	1	6
<50% (+)	10	22
<50% (−)	7	58
Sensitivity	0.94 (0.71–1.00)	0.73 (0.50–0.89)
Specificity	0.41 (0.18–0.67)	0.73 (0.61–0.82)
PPV	0.62 (0.41–0.80)	0.42 (0.26–0.59)
NPV	0.88 (0.47–1.00)	0.91 (0.81–0.97)
C-statistic	0.676	0.726

Values for sensitivity, specificity, PPV, and NPV presented with 95% confidence intervals.
CT = computed tomography; MPI = myocardial perfusion imaging; NPV = negative predictive value; PPV = positive predictive value; SPECT = single-photon emission computed tomography.

Feasibility of comprehensive CT protocol. Adenosine-enhanced stress CT was completed for all 34 patients within 27 ± 24 days after SPECT imaging. For 1 patient the rest and DE scans were not performed because of persisting angina after the adenosine DSCT stress examination.

Table 1 displays the scan parameters of each portion of the CT protocol. With the use of adenosine, the average heart rate increased from 68 ± 11 beats/min at rest to 79 ± 13 beats/min at stress, whereas the average heart rate variability (defined as maximum heart rate minus minimum heart rate during acquisition) decreased from 19 to 14 beats/min. Correspondingly, the average image quality was 3.4 ± 0.7 for rest scans and 3.1 ± 0.7 for stress scans ($p < 0.001$).

The average radiation exposure for the complete DSCT protocol was 12.7 ± 4.0 mSv and did not differ from SPECT (12.7 ± 0.4 mSv; $p = 0.99$) (Fig. 3).

CTA. Among the 34 CTA examinations, 11 (32%) patients had at least 1 nonevaluable segment. The most common reason for limited evaluation was the presence of extensive calcium. The average image quality for CTA was 2.5. Among the patients who had fully interpretable scans, 3 were normal, 4 had mild disease (≤40% stenosis), 4 had moderate disease (41% to 70% stenosis), and 12 (52%) had severe stenosis or an occluded vessel (>70% stenosis). When the nonevaluable segments were considered to represent severe disease, 23 (68%) patients were categorized as having severe CAD.

Diagnostic accuracy of CTA. When nonevaluable segments were considered to have significant disease, CTA had a sensitivity of 0.76 and 0.91 and specificity of 0.85 and 0.73 for detection of vessels with at least 50% and 70% stenosis,

Table 4 Diagnostic Accuracy of CTP With SPECT as Reference Standard for All Subjects (n = 34)

	CTP Stress Versus SPECT Stress	CTP Rest Versus SPECT Rest*
Left anterior descending		
Sensitivity	0.83 (0.52–0.98)	1.00 (0.48–1.00)
Specificity	0.64 (0.41–0.83)	0.72 (0.53–0.87)
PPV	0.56 (0.31–0.79)	0.39 (0.14–0.68)
NPV	0.88 (0.62–0.98)	1.00 (0.83–1.00)
C-statistic	0.735	0.857
Left circumflex artery		
Sensitivity	0.87 (0.60–0.98)	0.78 (0.40–0.97)
Specificity	0.84 (0.60–0.97)	0.79 (0.58–0.93)
PPV	0.81 (0.54–0.96)	0.58 (0.28–0.85)
NPV	0.89 (0.65–0.99)	0.91 (0.70–0.99)
C-statistic	0.854	0.785
Right coronary artery		
Sensitivity	0.82 (0.48–0.98)	0.67 (0.30–0.93)
Specificity	0.91 (0.72–0.99)	0.83 (0.63–0.95)
PPV	0.82 (0.48–0.98)	0.60 (0.26–0.88)
NPV	0.91 (0.72–0.99)	0.87 (0.66–0.97)
C-statistic	0.866	0.750
Per vascular territory	(n = 102) prevalence of stress perfusion defects = 0.37	(n = 99) prevalence of rest perfusion defects = 0.23
Sensitivity	0.84 (0.69–0.94)	0.78 (0.56–0.93)
Specificity	0.80 (0.68–0.89)	0.78 (0.67–0.86)
PPV	0.71 (0.56–0.84)	0.51 (0.34–0.69)
NPV	0.90 (0.79–0.96)	0.92 (0.83–0.97)
C-statistic	0.819	9.779

Values for sensitivity, specificity, PPV, and NPV presented with 95% confidence intervals.
*Includes 33 patients who completed the CT rest perfusion scan.
CTP = computed tomography perfusion; other abbreviations as in Table 3.

respectively. Correspondingly, the negative predictive value was 0.84 and 0.97 for excluding lesions with at least 50% and 70% stenosis.

When confining this analysis to only evaluable segments, the corresponding sensitivity, specificity, positive predictive value, and negative predictive value were 0.70, 0.94, 0.89, and 0.84, respectively, for detecting ≥50% stenosis and 0.88, 0.83, 0.54, and 0.97, respectively, for detecting ≥70% stenosis.

DSCT stress perfusion and SPECT MPI. Figures 4 and 5 illustrate examples of CT perfusion images and how they correlate to nuclear perfusion imaging. CT stress perfusion defects were identified for 26 of 34 patients (76%) and 45 of 102 vascular territories (44%). Of the 169 segments with adenosine-induced perfusion defects, 89 (53%) were graded as nontransmural, whereas the remaining 80 (47%) segments were graded as transmural. Of the 44 vascular territories with abnormal CT stress perfusion for which CT rest images were obtained, 11 (25%) were fixed, 12 (27%) were fully reversible, and 21 (48%) were partially reversible.

On a per-patient basis, CTP had a sensitivity of 0.92 and a specificity of 0.67 for the detection of stenosis ≥50% and a sensitivity of 0.94 and specificity of 0.41 for the detection of stenosis ≥70%. For the same patients, SPECT had an identical sensitivity and specificity for the detection of stenosis ≥50% and ≥70% (Table 3).

Table 3 shows the per-vessel diagnostic accuracy of CTP and SPECT among the 34 subjects included in the study. When stenosis of ≥50% on invasive angiography was used as the reference standard, the sensitivity and specificity were 0.79 and 0.80 for CTP and 0.67 and 0.83 for SPECT ($p = 0.10$ for differences in sensitivity, $p = 0.52$ for differences in specificity). On the other hand, when stenosis of ≥70% on invasive angiography was used as the reference standard, the sensitivity and specificity were 0.86 and 0.68 for CTP and 0.73 and 0.73 for SPECT ($p = 0.25$ for differences in sensitivity, $p = 0.32$ for differences in specificity). Thus, CTP showed equivalent sensitivity and specificity as compared with SPECT. Furthermore, for both modalities, when a reference standard of 70% was used rather than 50%, the sensitivity of perfusion for identifying anatomical stenosis increased and the specificity decreased. Consequently, the negative predictive values of excluding at least 70% stenosis were 0.95 for CTP and 0.91 for SPECT.

There was no significant difference when comparing the C-statistic (equal to the area under the receiver-operator characteristics curve) with SPECT and CTP for discriminating between patients with and without significant stenosis.

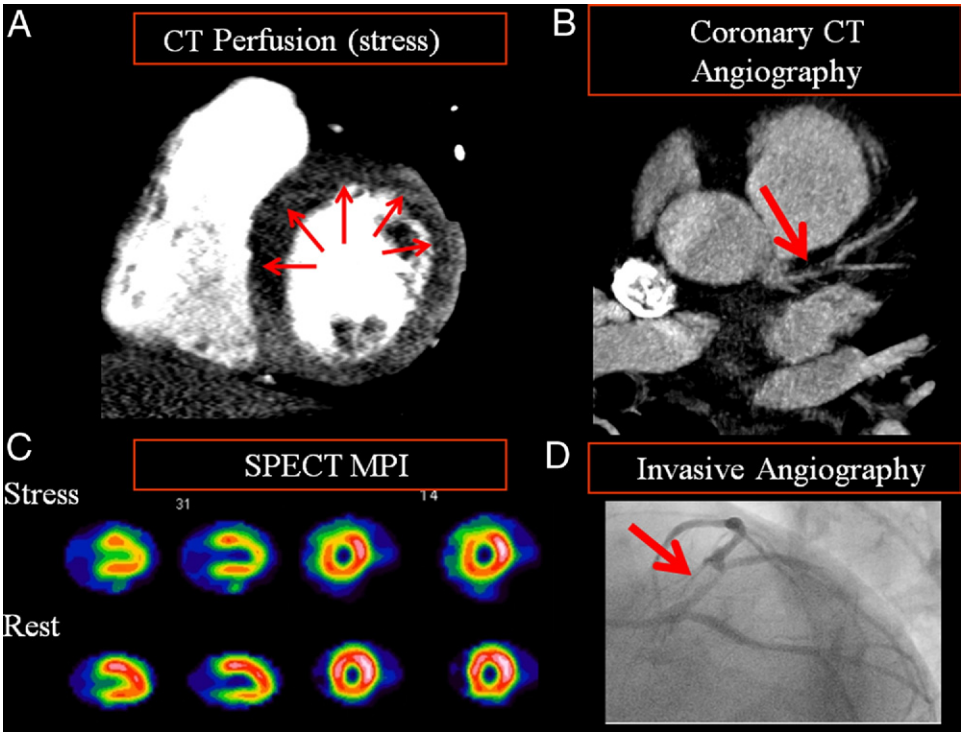

Figure 4 **Example of Single-Vessel Disease Identified by All Modalities**

A 59-year-old obese man with no prior cardiac history who presented with chest pain and dyspnea on exertion. A CT perfusion showed a large perfusion defect in the anteroseptal, anterior, and anterolateral walls **(A)**. **(B)** The CT angiography showed large noncalcified plaque in the proximal LAD; **(C)** SPECT MPI images with fully reversible defect throughout the mid and apical anterior wall. **(D)** Invasive angiography in the left anterior oblique caudal view showing severe stenosis in LAD before the takeoff of the first diagonal branch. LAD = left anterior descending; other abbreviations as in Figure 3.

JACC Vol. 54, No. 12, 2009
September 15, 2009:1072–84

When the reference standard was defined as vessels that had both stenosis ≥50% and a corresponding SPECT perfusion abnormality, CTP had a sensitivity of 0.93 and specificity of 0.74. On the other hand, when the reference was defined to include all vessels with either stenosis ≥50% or a corresponding SPECT perfusion abnormality, CTP had a sensitivity of 0.75 and a specificity of 0.88.

DSCT stress and rest perfusion using SPECT MPI as a reference. Table 4 provides the diagnostic accuracy of stress and rest CTP to identify perfusion defects using SPECT imaging as the reference standard. On a per vascular territory basis, stress CT had a reasonable accuracy in identifying defects visualized on stress nuclear MPI. Similarly, perfusion defects identified on rest CT identified rest nuclear MPI defects, although the accuracy of rest CT seemed to be better for defects in the left anterior descending distribution than those present in the right coronary artery or left circumflex distribution.

DE. Myocardial DE was visualized in 17 of the 33 patients who completed the protocol (see example in Fig. 6). The quality of DE images was 2.8 ± 0.8 and was significantly lower than the corresponding score for the stress or rest images. On a per patient level, the accuracy of CT DE to detect resting perfusion defects on SPECT was good, with a sensitivity of 0.82, specificity of 0.81, positive predictive value of 0.82, and negative predictive value of 0.81. When this comparison was confined to the 16 DE scans that were thought to have good or excellent quality (i.e., image quality score ≥3), the sensitivity was 1.00 and the specificity was 0.89. All 17 patients who had evidence of DE had rest CTP defects; however, there were 4 patients who had rest perfusion defects who did not have any evidence of DE. In all of these cases the rest perfusion defects were nontransmural. In addition, none of these 4 patients had a history of MI or percutaneous coronary intervention, and none of these 4 patients had any perfusion defects on rest nuclear perfusion imaging.

Discussion

In one of the first human studies of adenosine-mediated stress DSCT, we showed the feasibility of a novel cardiac CT protocol that combines stress and rest MPI together with coronary CTA in a single examination. Furthermore, we showed that CT stress MPI has comparable diagnostic accuracy to SPECT in detecting hemodynamically significant stenosis. Importantly, in this comprehensive CT protocol information on coronary anatomy, stress perfusion, rest perfusion, function, and DE was available with an average radiation exposure that was equivalent to SPECT.

Nuclear perfusion imaging has revolutionized the field of cardiovascular imaging because it has allowed for an accurate noninvasive method to detect physiologically significant

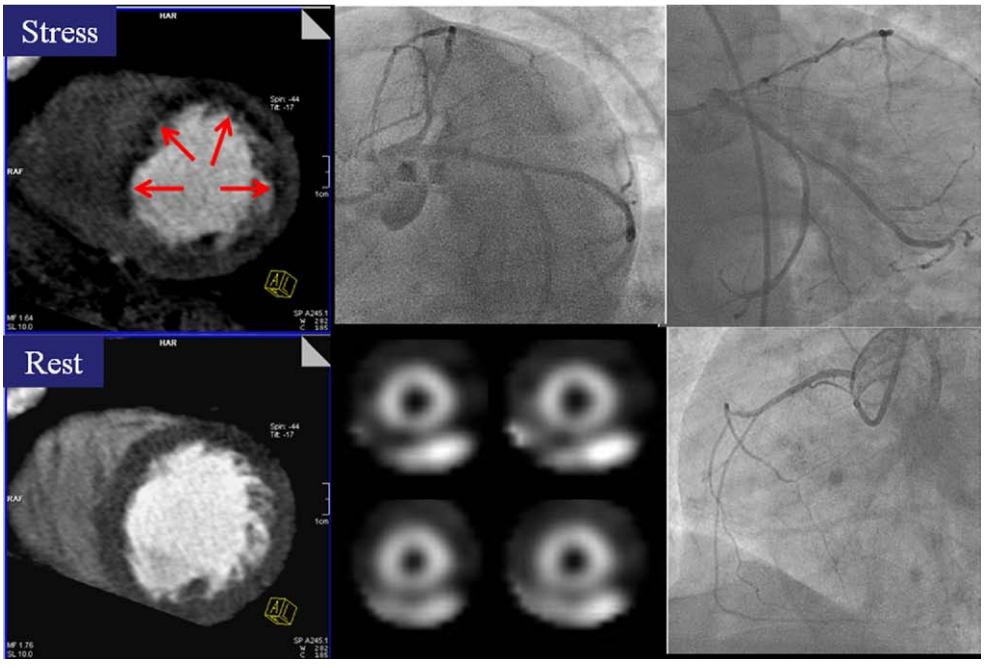

Figure 5 **Example of CT Perfusion Identifying Multivessel Disease**

A 60-year-old man with diabetes, dyslipidemia, hypertension, and a prior LAD stent who presented with chest pain. The CT perfusion **(arrows)** showed a perfusion defect throughout the anteroseptum, anterior, anterolateral, and inferolateral segments. On invasive angiography, the patient had severe disease in the proximal LAD and moderate stenosis in the left circumflex vessel. The SPECT study was read as normal with attenuation-related artifact in the inferior wall. It is likely that the apparently normal SPECT was caused by balanced myocardial ischemia. Abbreviations as in Figures 3 and 4.

CAD while simultaneously providing robust prognostic information that can help determine the need for further patient management. Importantly, in appropriately selected patients, nuclear MPI has been shown to be an efficient and cost-effective strategy that can avoid the use of unnecessary invasive angiography (19). Nevertheless, SPECT MPI has limitations because attenuation artifacts can lead to false-positive findings while balanced ischemia in the setting of multivessel disease may result in false negatives. Given these considerations, a test that can provide both anatomical visualization of coronary stenosis together with an accurate physiological assessment of perfusion would be beneficial. Although our study only represents a limited experience, it suggests that CT could have an important role as a modality that would be able to simultaneously assess both anatomical CAD and its physiological consequences.

CTP: pros and cons. An important advantage of CTP is the ability to simultaneously visualize both coronary anatomy and myocardial perfusion. In comparison to SPECT, CT has improved spatial resolution and may be better at detecting small areas of ischemia or infarction. Furthermore, CTP could offer improved accuracy for detecting multivessel disease because actual rather than relative blood flow patterns are assessed, thus avoiding false negatives that can occur in the setting of balanced myocardial ischemia. However, there are several limitations that are pertinent to CTP. First, as is also the case with nuclear-based perfusion imaging, patients are exposed to ionizing radiation. Although in our study the total effective dose was equal for SPECT and CT, the distribution of the dose among the different organs in the body will differ (20). Second, in comparison to regular CTA, a larger volume of iodinated contrast is required as both rest and stress images are acquired. Third, there are artifacts, such as motion and beam hardening, that are unique to CT-based perfusion imaging.

Comparing anatomy and perfusion. There are several potential mechanisms that could explain minor discrepancies between the CTP findings and invasive angiography. For instance, some patients with previous myocardial infarction had perfusion defects but nonobstructive coronary anatomy (e.g., post-percutaneous coronary intervention or after a thrombus that spontaneously recanalized). In another case, a circumferential subendocardial perfusion defect was present during stress CT, although both invasive angiography and SPECT were negative (Fig. 7). In this particular case, although all 3 vascular territories were classified as having a false-positive CTP, we suspect that microvascular disease was present and caused the apparent defect. The defect was not visualized with SPECT because it has a lower spatial resolution than CT. Given that in some subgroups of patients, the presence of microvascular disease (i.e., syndrome X) is associated with worse prognosis

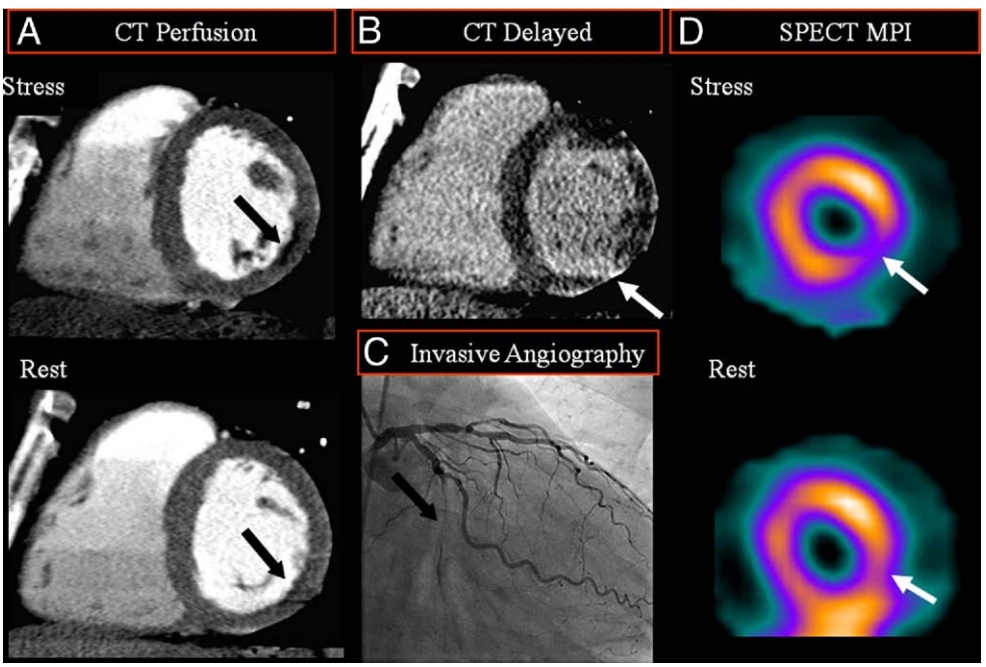

Figure 6 **Example of Peri-Infarct Ischemia**

A 63-year-old man with diabetes mellitus, hypertension, dyslipidemia, and prior myocardial infarction presented with near syncope. The CT perfusion **(A)** during adenosine infusion revealed a focal perfusion defect in the mid inferolateral segment. The rest CT showed a very small subendocardial perfusion defect in the same territory. Delayed-enhancement CT **(B)** showed subendocardial delayed enhancement along the inferolateral wall consistent with prior infarction in this region, smaller than the stress perfusion defect. On invasive angiography (**C**; right anterior oblique caudal projection), the patient had a subtotal occlusion of the mid left circumflex coronary artery. Nuclear SPECT imaging **(D)** also showed a small infarct in the inferolateral wall with peri-infarct ischemia. Abbreviations as in Figure 3.

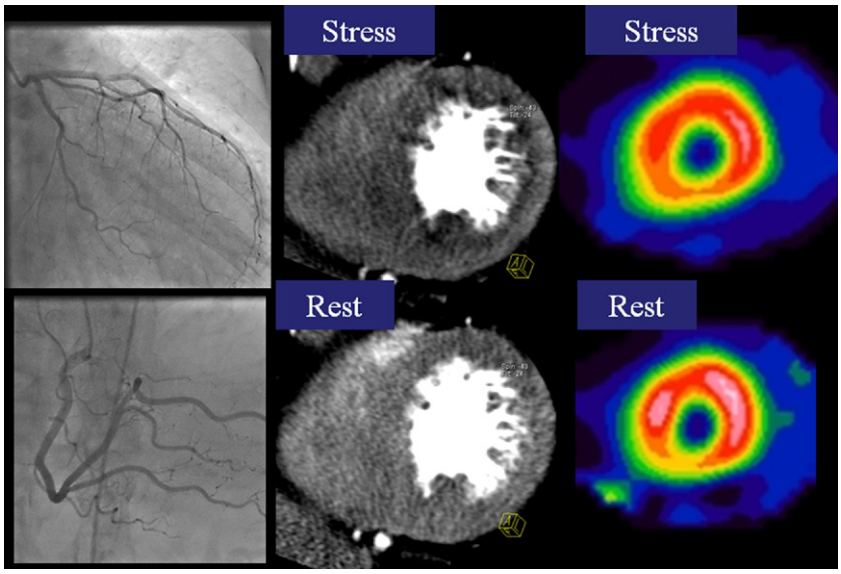

Figure 7 **Example of False-Positive CT Perfusion**

An 84-year-old man with hypertension, dyslipidemia, and tobacco use who presented with pre-syncope. Evaluation of CT myocardial perfusion during adenosine infusion showed a circumferential subendocardial perfusion defect that on blinded reading was thought to represent multivessel disease. The SPECT MPI and invasive angiography did not reveal any significant disease. Given that the patient has multiple risk factors for microvascular disease, it is possible that the perfusion abnormalities identified in this case are consistent with microvascular disease in the absence of significant epicardial coronary artery disease. Abbreviations as in Figure 3.

(21,22), it may be important to recognize such findings. Finally, some defects visualized on CTP correlated with <50% stenosis on quantitative coronary assessment and were classified as false positive. Such cases serve as a reminder that the correlation between physiological significance of coronary disease and luminal stenosis is not perfect.

Stress coronary CTA. Despite the increased heart rate observed during adenosine administration, the absence of nitroglycerin, and the large extent of calcified plaque in our patient population, we observed a reasonable accuracy of stress coronary CTA. That similar accuracy has been reported for rest CTA (23) implies that even during adenosine administration, it is still feasible to accurately identify anatomical stenosis with CTA. Given the higher temporal resolution associated with the DSCT, it remains to be seen whether this finding can also be validated in other scanners.

CT DE. An additional aspect of our comprehensive protocol is that DE imaging was used. Although previous studies have shown the ability of CT DE to identify areas of prior myocardial infarction (24–26), none of these studies were performed as part of a stress perfusion protocol. In our study the added radiation dose of DE imaging was very low (average 1.2 mSv); however, the image quality of DE was significantly lower than both the stress and the rest examinations. In our protocol, DE was used together with the rest images to differentiate reversible from nonreversible ischemia; however, because rest perfusion defects were present for all patients who had DE, the added value of DE is uncertain. Thus, it remains to be seen if CT DE imaging adds additional information over CT rest perfusion imaging to be routinely incorporated as part of future stress perfusion protocols.

Anticipated technological advances. Future technological advances in CT may enhance the diagnostic accuracy of CTP. Specifically, such improvements may include: 1) improved temporal resolution, which may reduce motion artifacts that are seen during increased heart rate induced by adenosine; 2) improved coverage in the z-axis, which may reduce slab and misregistration artifacts; 3) improved spatial resolution; and 4) improved reconstruction algorithms, for instance, iterative reconstruction algorithms may lead to further optimizing the signal-to-noise and contrast-to-noise ratios, improve resolution, and may be more resilient to motion artifacts.

Study limitations. First, this is a single-center study, and thus it would be important to validate these results in other centers and in a multicenter fashion. Second, the assessment of nuclear perfusion studies in our study is somewhat limited by the fact that some patients had a suboptimal workload, which could result in reduced sensitivity of the SPECT MPI examination. Our study included patients with both known and suspected CAD. Although the inclusion of patients with known disease allowed us to investigate the use of perfusion imaging for detecting areas of infarction and ischemia, this also may present several dilemmas. For instance, patients who underwent a previous percutaneous revascularization in the setting of MI may have patent coronary arteries (caused by the presence of a stent) yet have infarcted myocardium. Nevertheless, CAD is

a complex disease and many patients who present for an evaluation of suspected CAD have previously known disease. As such, it is important for any modality to be able to accurately evaluate such patients.

Although the primary aim of our study was to assess the feasibility of a comprehensive CT protocol using vasodilator stress, we also reported and compared the diagnostic accuracy of CTP to SPECT MPI. In doing so, it is important to note that our study design is prone to selection and verification bias. Selection bias may be present in our design because recruited subjects generally had high-risk features on SPECT imaging. As such, many patients (but not all) had positive perfusion defects on SPECT MPI. This could bias the results toward higher false positives in the SPECT group; however, we found that false positives were slightly more common for CTP.

Finally, we showed that cardiac CT has an important potential future role in MPI for detection of myocardial ischemia. However, based on our single-center experience, at this time this technique should only be used as an investigational tool. Although future studies are needed to further define the diagnostic accuracy of combining CTA and CTP, in patients already undergoing cardiac CT for evaluation of coronary anatomy, rest perfusion defects, when present, can be very helpful in identifying areas of infarcted myocardium. Current and future research involving stress perfusion and DE will further define the future role of these developing techniques for the identification of ischemic and infarcted myocardium, respectively.

Acknowledgments

The authors thank the CT technologists and the Radiology Department nursing staff as well as the many cardiologists who assisted with this study at the Massachusetts General Hospital.

Reprint requests and correspondence: Dr. Ron Blankstein, Cardiac MR PET CT Program, Department of Radiology and Division of Cardiology, Massachusetts General Hospital, 165 Cambridge Street, Suite 400, Boston, Massachusetts 02114. E-mail: rblankstein@partners.org.

REFERENCES

1. Meijboom WB, Van Mieghem CA, van Pelt N, et al. Comprehensive assessment of coronary artery stenoses: computed tomography coronary angiography versus conventional coronary angiography and correlation with fractional flow reserve in patients with stable angina. J Am Coll Cardiol 2008;52:636–43.
2. Hachamovitch R, Berman DS, Shaw LJ, et al. Incremental prognostic value of myocardial perfusion single photon emission computed tomography for the prediction of cardiac death: differential stratification for risk of cardiac death and myocardial infarction. Circulation 1998;97:535–43.
3. Hachamovitch R, Hayes SW, Friedman JD, Cohen I, Berman DS. Comparison of the short-term survival benefit associated with revascularization compared with medical therapy in patients with no prior coronary artery disease undergoing stress myocardial perfusion single photon emission computed tomography. Circulation 2003;107:2900–7.
4. Di Carli MF, Dorbala S, Curillova Z, et al. Relationship between CT coronary angiography and stress perfusion imaging in patients with suspected ischemic heart disease assessed by integrated PET-CT imaging. J Nucl Cardiol 2007;14:799–809.
5. Di Carli MF, Hachamovitch R. Hybrid PET/CT is greater than the sum of its parts. J Nucl Cardiol 2008;15:118–22.
6. Cury RC, Nieman K, Shapiro MD, et al. Comprehensive assessment of myocardial perfusion defects, regional wall motion, and left ventricular function by using 64-section multidetector CT. Radiology 2008;248:466–75.
7. Hoffmann U, Millea R, Enzweiler C, et al. Acute myocardial infarction: contrast-enhanced multi-detector row CT in a porcine model. Radiology 2004;231:697–701.
8. Mahnken AH, Bruners P, Katoh M, Wildberger JE, Gunther RW, Buecker A. Dynamic multi-section CT imaging in acute myocardial infarction: preliminary animal experience. Eur Radiol 2006;16:746–52.
9. Nieman K, Shapiro MD, Ferencik M, et al. Reperfused myocardial infarction: contrast-enhanced 64-section CT in comparison to MR imaging. Radiology 2008;247:49–56.
10. Ruzsics B, Lee H, Zwerner PL, Gebregziabher M, Costello P, Schoepf UJ. Dual-energy CT of the heart for diagnosing coronary artery stenosis and myocardial ischemia-initial experience. Eur Radiol 2008;18:2414–24.
11. Gerber BL, Belge B, Legros GJ, et al. Characterization of acute and chronic myocardial infarcts by multidetector computed tomography: comparison with contrast-enhanced magnetic resonance. Circulation 2006;113:823–33.
12. George RT, Jerosch-Herold M, Silva C, et al. Quantification of myocardial perfusion using dynamic 64-detector computed tomography. Invest Radiol 2007;42:815–22.
13. George RT, Silva C, Cordeiro MA, et al. Multidetector computed tomography myocardial perfusion imaging during adenosine stress. J Am Coll Cardiol 2006;48:153–60.
14. Kurata A, Mochizuki T, Koyama Y, et al. Myocardial perfusion imaging using adenosine triphosphate stress multi-slice spiral computed tomography: alternative to stress myocardial perfusion scintigraphy. Circ J 2005;69:550–7.
15. Zoghbi GJ, Dorfman TA, Iskandrian AE. The effects of medications on myocardial perfusion. J Am Coll Cardiol 2008;52:401–16.
16. Blankstein R, Shah A, Pale R, et al. Radiation dose and image quality of prospective triggering with dual-source cardiac computed tomography. Am J Cardiol 2009;103:1168–73.
17. Cerqueira MD, Weissman NJ, Dilsizian V, et al. Standardized myocardial segmentation and nomenclature for tomographic imaging of the heart: a statement for healthcare professionals from the Cardiac Imaging Committee of the Council on Clinical Cardiology of the American Heart Association. Circulation 2002;105:539–42.
18. Blankstein R, Rogers IS, Cury RC. Practical tips and tricks in cardiovascular computed tomography: diagnosis of myocardial infarction. J Cardiovasc Comput Tomogr 2009;3:104–11.
19. Shaw LJ, Hachamovitch R, Berman DS, et al., for the Economics of Noninvasive Diagnosis (END) Multicenter Study Group. The economic consequences of available diagnostic and prognostic strategies for the evaluation of stable angina patients: an observational assessment of the value of precatheterization ischemia. J Am Coll Cardiol 1999;33:661–9.
20. Einstein AJ, Moser KW, Thompson RC, Cerqueira MD, Henzlova MJ. Radiation dose to patients from cardiac diagnostic imaging. Circulation 2007;116:1290–305.
21. Johnson BD, Shaw LJ, Buchthal SD, et al. Prognosis in women with myocardial ischemia in the absence of obstructive coronary disease: results from the National Institutes of Health-National Heart, Lung, and Blood Institute-Sponsored Women's Ischemia Syndrome Evaluation (WISE). Circulation 2004;109:2993–9.
22. Johnson BD, Shaw LJ, Pepine CJ, et al. Persistent chest pain predicts cardiovascular events in women without obstructive coronary artery disease: results from the NIH-NHLBI-sponsored Women's Ischaemia Syndrome Evaluation (WISE) study. Eur Heart J 2006;27:1408–15.
23. Budoff MJ, Dowe D, Jollis JG, et al. Diagnostic performance of 64-multidetector row coronary computed tomographic angiography for evaluation of coronary artery stenosis in individuals without known coronary artery disease: results from the prospective multicenter ACCURACY (Assessment by Coronary Computed Tomographic

Angiography of Individuals Undergoing Invasive Coronary Angiography) trial. J Am Coll Cardiol 2008;52:1724–32.
24. Baks T, Cademartiri F, Moelker AD, et al. Assessment of acute reperfused myocardial infarction with delayed enhancement 64-MDCT. AJR Am J Roentgenol 2007;188:W135–7.
25. le Polain de Waroux JB, Pouleur AC, Goffinet C, Pasquet A, Vanoverschelde JL, Gerber BL. Combined coronary and late-enhanced multidetector-computed tomography for delineation of the etiology of left ventricular dysfunction: comparison with coronary angiography and contrast-enhanced cardiac magnetic resonance imaging. Eur Heart J 2008;29:2544–51.
26. Mahnken AH, Bruners P, Muhlenbruch G, et al. Low tube voltage improves computed tomography imaging of delayed myocardial contrast enhancement in an experimental acute myocardial infarction model. Invest Radiol 2007;42:123–9.

Key Words: infarction ■ ischemia ■ imaging ■ coronary disease ■ computed tomography.